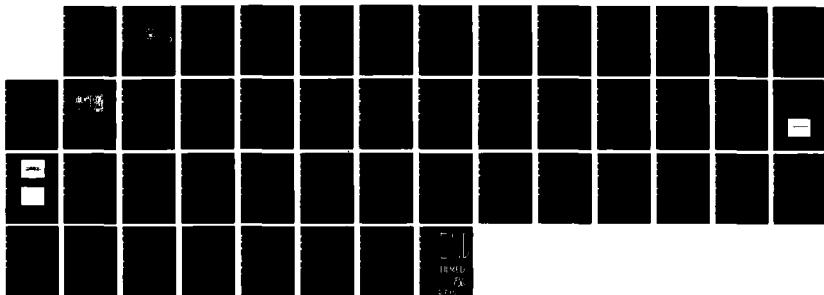
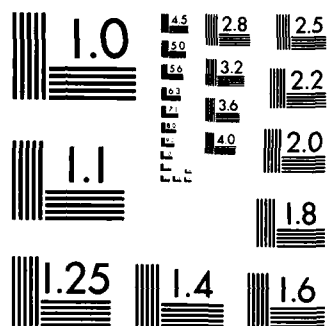


ANALYSIS OF CONTRAST SENSITIVITY AND SPECTRAL RESPONSE  
OF IMAGING SYSTEMS(U) NAVAL POSTGRADUATE SCHOOL  
MONTEREY CA Y 5 KIM DEC 85

F/G 9/1

NL





MICROCOPY RESOLUTION TEST CHART  
 NATIONAL BUREAU OF STANDARDS-1963-A

2

# NAVAL POSTGRADUATE SCHOOL

Monterey, California

AD-A164 228



DTIC  
ELECTE  
FEB 14 1986  
S B D

## THESIS

ANALYSIS OF CONTRAST SENSITIVITY AND  
SPECTRAL RESPONSE OF IMAGING SYSTEMS

by

Young Soo Kim

December 1985

Thesis Advisor:

Edmund A. Milne

Approved for public release; distribution is unlimited.

DTIC FILE COPY

86 2 14 074

## REPORT DOCUMENTATION PAGE

1a. REPORT SECURITY CLASSIFICATION			1b. RESTRICTIVE MARKINGS		
2a. SECURITY CLASSIFICATION AUTHORITY			3. DISTRIBUTION/AVAILABILITY OF REPORT Approved for public release; distribution is unlimited.		
2b. DECLASSIFICATION/DOWNGRADING SCHEDULE					
4. PERFORMING ORGANIZATION REPORT NUMBER(S)			5. MONITORING ORGANIZATION REPORT NUMBER(S)		
6a. NAME OF PERFORMING ORGANIZATION Naval Postgraduate School		6b. OFFICE SYMBOL (if applicable) 61		7a. NAME OF MONITORING ORGANIZATION Naval Postgraduate School	
6c. ADDRESS (City, State, and ZIP Code) Monterey, California 93943-5100				7b. ADDRESS (City, State, and ZIP Code) Monterey, California 93943-5100	
8a. NAME OF FUNDING/SPONSORING ORGANIZATION		8b. OFFICE SYMBOL (if applicable)		9. PROCUREMENT INSTRUMENT IDENTIFICATION NUMBER	
8c. ADDRESS (City, State, and ZIP Code)				10. SOURCE OF FUNDING NUMBERS	
				PROGRAM ELEMENT NO.	PROJECT NO.
11. TITLE (Include Security Classification) ANALYSIS OF CONTRAST SENSITIVITY AND SPECTRAL RESPONSE OF IMAGING SYSTEMS					
12. PERSONAL AUTHOR(S) Kim, Young Soo					
13a. TYPE OF REPORT Master's Thesis		13b. TIME COVERED FROM TO		14. DATE OF REPORT (Year, Month, Day) 1985 December	
15. PAGE COUNT 47					
16. SUPPLEMENTARY NOTATION					
17. COSATI CODES			18. SUBJECT TERMS (Continue on reverse if necessary and identify by block number) CID, CCD, VIDICON, Noise, Limiting Resolution, Contrast Sensitivity, Spectral Response		
FIELD	GROUP	SUB-GROUP			
19. ABSTRACT (Continue on reverse if necessary and identify by block number) <p>The characteristics of imaging systems CID, CCD, and VIDICON were investigated in terms of the contrast sensitivity and the spectral response in the near infrared region. The object distance of 83.5cm, the radiant flux density of 0.93 microwatts/cm<sup>2</sup> and a black and white bar chart were used for the measurement of CTF. The spectral response was measured at 2520 °K using a tungsten light source. The CID image sensor has high sensitivity, resolving capability and spectral response at low light level comparing to the CCD or VIDICON. The limiting resolution values of 23.0 line-pairs/mm for CCD and 28.4 line-pairs/mm for VIDICON, the cutoff wavelengths of 1.0 micrometers for CCD and 0.94 micrometers for VIDICON were determined. The limiting resolution value and the cutoff wavelength for CID were much higher than those of CCD or VIDICON and lay outside the range of this experiment.</p>					
20. DISTRIBUTION/AVAILABILITY OF ABSTRACT <input checked="" type="checkbox"/> UNCLASSIFIED/UNLIMITED <input type="checkbox"/> SAME AS RPT. <input type="checkbox"/> DTIC USERS				21. ABSTRACT SECURITY CLASSIFICATION unclassified	
22a. NAME OF RESPONSIBLE INDIVIDUAL Edmund A. Milne				22b. TELEPHONE (Include Area Code) (408) 646-2886	
				22c. OFFICE SYMBOL 61Mn	

Approved for public release; distribution is unlimited.

Analysis of Contrast Sensitivity and  
Spectral Response of Imaging Systems

by

Young Soo Kim  
Lieutenant, Korean Navy  
B.S., Korea Naval Academy, 1978

Submitted in partial fulfillment of the  
requirements for the degree of

MASTER OF SCIENCE IN PHYSICS

from the

NAVAL POSTGRADUATE SCHOOL  
December 1985

Author:

*Young Soo Kim*

Young Soo Kim

Approved by:

*Edmund A. Milne*

Edmund A. Milne, Thesis Advisor

*Alfred W. Cooper*

Alfred W. Cooper, Second Reader

*Gordon E. Schacher*

Gordon E. Schacher, Chairman,  
Department of Physics

*John N. Dyer*

John N. Dyer,  
Dean of Science and Engineering

# ABSTRACT

The characteristics of imaging systems CID, CCD and VIDICON were investigated in terms of the contrast sensitivity and the spectral response in the near infrared region. The object distance of 83.5cm, the radiant flux density of 0.93 microwatts/cm<sup>2</sup> and a black and white bar chart were used for the measurement of CTF. The spectral response was measured at 2520 °K using a tungsten light source. The CID image sensor has high sensitivity, resolving capability and spectral response at low light level comparing to the CCD or VIDICON. The limiting resolution values of 23.0 line-pairs/mm for CCD and 28.4 line-pairs/mm for VIDICON, the cutoff wavelengths of 1.0 micrometers for CCD and 0.94 micrometers for VIDICON were determined. The limiting resolution value and the cutoff wavelength for CID were much higher than those of CCD or VIDICON and lay outside the range of this experiment.

Accession For	
NTIS GRA&I	<input checked="" type="checkbox"/>
DTIC TAB	<input type="checkbox"/>
Unannounced	<input type="checkbox"/>
Justification	
By	
Distribution/	
Availability Codes	
Dist	Avail and/or Special
A-1	

## TABLE OF CONTENTS

I.	INTRODUCTION . . . . .	8
II.	THEORETICAL CONSIDERATIONS . . . . .	10
	A. GENERAL . . . . .	10
	B. CONTRAST TRANSFER FUNCTION (CTF) . . . . .	10
	C. SPECTRAL RESPONSE . . . . .	14
III.	EXPERIMENTAL MEASUREMENTS AND RESULTS . . . . .	21
	A. EXPERIMENTAL APPARATUS . . . . .	21
	B. CONTRAST SENSITIVITY . . . . .	24
	1. Signal-to-Noise Ratio (SNR) . . . . .	24
	2. Dynamic Range . . . . .	27
	3. Linearity . . . . .	28
	4. Contrast Transfer Function (CTF) . . . . .	31
	C. SPECTRAL RESPONSE . . . . .	35
	1. Spectral Radiant Emittance . . . . .	35
	2. Responsivity of TV Camera . . . . .	36
IV.	CONCLUSIONS . . . . .	45
	LIST OF REFERENCES . . . . .	46
	INITIAL DISTRIBUTION LIST . . . . .	47

## LIST OF TABLES

I	MAXIMUM SIGNAL-TO-NOISE RATIO . . . . .	27
II	DYNAMIC RANGE COMPARISON . . . . .	27
III	THE VISIBLE LINES IN THE SPECTRUM OF A MERCURY ARC . . . . .	35



## LIST OF FIGURES

2.1	Geometry for Spatial Frequency . . . . .	12
2.2	Standard Method of Determining SNR . . . . .	13
2.3	Elements of Spectroradiometer . . . . .	15
2.4	Diffraction Grating and Imager Array Pixels . . . . .	16
2.5	Geometry of Angle for Obliquity Factor . . . . .	18
3.1	Spectral Response Measurement Set-up . . . . .	22
3.2	Transmittance of the IR Filter . . . . .	23
3.3	Noise without a Signal(50mV/div): CID . . . . .	25
3.4	Noise without a Signal(50mV/div): CCD . . . . .	26
3.5	Noise without a Signal(50mV/div): VIDICON . . . . .	26
3.6	The Maximum Output Voltage vs F Number . . . . .	29
3.7	Linearity of TV Camera Signal . . . . .	30
3.8	CTF for CID at F=4.0 and O=83.5 cm . . . . .	32
3.9	CTF for CCD at F=1.4 and O=83.5 cm . . . . .	33
3.10	CTF for VIDICON at F=1.4 and O=83.5 cm . . . . .	34
3.11	Tungsten Lamp Emissivity (T=2520 °K) . . . . .	38
3.12	Blackbody Spectral Radiant Emittance (T=2520 °K) . . . . .	40
3.13	Tungsten Spectral Radiant Emittance (T=2520 °K) . . . . .	41
3.14	Deflection Angle vs Wavelength . . . . .	42
3.15	Signal Output vs Wavelength . . . . .	43
3.16	Responsivity of TV Camera . . . . .	44

#### ACKNOWLEDGEMENTS

I wish to express my appreciation to Mr. Robert Sanders for his technical support and devotion of his time in the execution of this research.

I express special thanks to professor Edmund Alexander Milne whose wisdom and guidance were invaluable in the preparation of this thesis.

Finally, I would like to thank my wife, Soo Ok, for her love, enduring and sharing pressure and the loneliness.

## I. INTRODUCTION

Infrared imaging systems can be used for medical diagnosis, night vision, real-time aircraft reconnaissance, commercial TV broadcasting, military and other surveillance applications.

In recent years, however, great effort has gone into the development of sensors to operate under extremely low illumination conditions for security and surveillance purposes and has also been pushing in the direction of extending the spectral responsivity into the infrared.

A common problem in electro-optics is the detection and resolution of detail in the presence of noise. It is common practice to specify the resolving capability of an electro-optical imaging system in terms of the image of a black and white bar chart [Ref. 1: p.109].

The Modulation Transfer Function(MTF) or the Contrast Transfer Function (CTF) characteristics are preferable ways of specifying TV camera tube resolution. The limiting resolution values for 100% contrast of target provide only a single point on the CTF characteristic curve which is the spatial frequency where the CTF has fallen to a value of three percent. With actual scene contrast values of 30 percent, or less, the resolution is considerably reduced below that for 100% contrast [Ref. 1: p.201].

A VIDICON is the most widely used camera tube. The speed of response is somewhat less than that of most other types of camera tubes. The VIDICON utilizes an electron beam to scan a photoconductive target which is the light sensor. When a light pattern is focused on the photoconductor, its conductivity increases in the illuminated areas and the back side of the target becomes more positive.

The electron beam then reads the signal by depositing electrons on the positively charged areas thereby providing a capacitively coupled signal at the signal electrode.

A charge-coupled device (CCD) is metal-oxide-semiconductor (MOS) type solid-state imaging device which requires no scanning beam. The charges, representing picture-element signals, are stored in potential wells under depletion-biased electrodes. The charges are transferred by applying a positive pulse to the adjacent electrodes. The whole image is transferred, in this manner to a storage raster during the vertical blanking period. Each horizontal line is then readout from the storage raster in sequence in a similar manner to provide the output TV signal.

A charge-injection device (CID) image sensor employs intra-cell transfer and injection to sense photon-generated charge at each sensing site. The level of signal charge at each sensing site is detected during a line scan, and during the retrace interval, all charge in the selected line is injected. The injection operation is used to reset the charge storage capacitors after line readout has been completed. A video signal can be created by injecting the stored charge into the substrate (sequential injection) or by injecting in parallel at all sites in the addressed row (parallel injection). A performance and some characteristics of the imagers were described in detail [Ref. 2,3,4].

In this paper, the characteristics of TV camera tubes of CCD, CID and VIDICON type have been examined based on experimental measurements of contrast sensitivity and spectral response. A black and white bar chart, a tektronix 468 digital storage oscilloscope, a spectrometer and a tungsten light source were used for these measurements.

## II. THEORETICAL CONSIDERATIONS

### A. GENERAL

The TV camera tubes are used to generate a train of electrical pulses which represent light intensities in an optical image focused on the tube. This section provides a general discussion and theoretical outline of CTF and spectral response in the near infrared region of three TV camera tubes.

### B. CONTRAST TRANSFER FUNCTION (CTF)

The resolution is often described by the limiting line spacing on a bar chart which can be resolved in the image. The resolution performance of an imaging system can be measured in terms of CTF, the square wave spatial frequency amplitude response, as function of spatial frequency.

The CTF can be constructed by line analysis of a TV picture of the black and white bar chart. the CTF may be defined as the ratio of amplitude difference of the image output signal between the background and the dark bar to the sum of it which can be written as

$$CTF = \frac{V_{max} - V_{min}}{V_{max} + V_{min}} \quad (\text{eqn 2.1})$$

where  $V_{max}$  is the maximum amplitude of the image output signal due to the bright background and  $V_{min}$  is the minimum amplitude of the image output signal due to the dark bar.

The consideration of noise and dynamic range will follow that of image spatial frequency.

The image spatial frequency is found by calculating the object spatial frequency,  $f_{so}$ , and image magnification,  $m$ , defined as

$$f_{so} = n/d \quad (\text{eqn 2.2})$$

$$m = I/O \quad (\text{eqn 2.3})$$

where

$n$  = number of line-pairs of object (line-pairs)

$d$  = width of object (mm)

$I$  = image distance from lens (mm)

$O$  = object distance from lens (mm).

Since the image distance must be determined by the object distance and the focal length of the lens, it can be written as

$$I = \frac{Of}{O - f} \quad (\text{eqn 2.4})$$

for the thin lens, where  $f$  is the focal length of the lens.

Substituting equation 2.4 back into equation 2.3 we get the image spatial frequency  $f_s$  as

$$f_s = \frac{f}{m} = \frac{nO}{Id} = \frac{n(O - f)}{fd} \quad (\text{eqn 2.5})$$

This is shown geometrically in Figure 2.1. An important parameter affecting the amplitude of the image output signal is the noise of the imager since it determines the sensitivity of the device and greatly affects the dynamic range.

The rms (root mean square) value of the noise may be approximated by the standard deviation value of the noise which can be determined from the measured samples of the individual fluctuation using the formula with grouped data given by Ref. 5

$$S = \left[ \frac{n \sum_{i=1}^k x_i^2 f_i - \left( \sum_{i=1}^k x_i f_i \right)^2}{n(n-1)} \right]^{\frac{1}{2}} \quad (\text{eqn 2.6})$$

where

- s = standard deviation of the noise
- n = number of measured sample (sample size)
- x = class mark
- f = frequency of the sample.

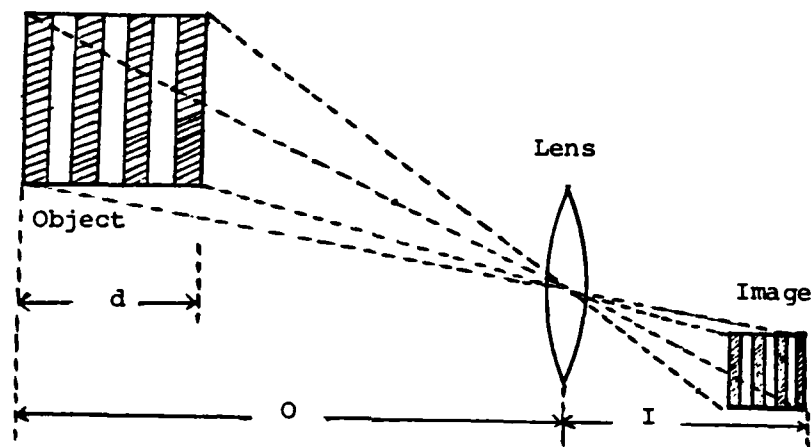


Figure 2.1 Geometry for Spatial Frequency.

The rms noise determines the signal-to-noise ratio( SNR) and the dynamic range of the imaging system.

An infrared imaging device records a signal that is proportional to the power on the detector for a thermal detector, and to the number of photons per unit time for a photon detector.

The television video signal in every piece of practical television camera equipment contains a significant random fluctuation or noise current, and this noise current acts to limit picture quality, especially at low input light levels or at low scene contrasts. Since the eye can see contrasts only down to 3-5%, the apparent peak-to-peak noise envelope represents the  $\pm 3\sigma$  points of the noise pulse distribution where  $\sigma$  is the standard deviation of the noise amplitude

distribution. Hence the rms noise current may be approximated as 1/6 the apparent peak-to-peak current envelope. Standard method of determining signal-to-noise ratio for television camera tubes is well described in Ref. 6 and showed in Figure 2.2 .

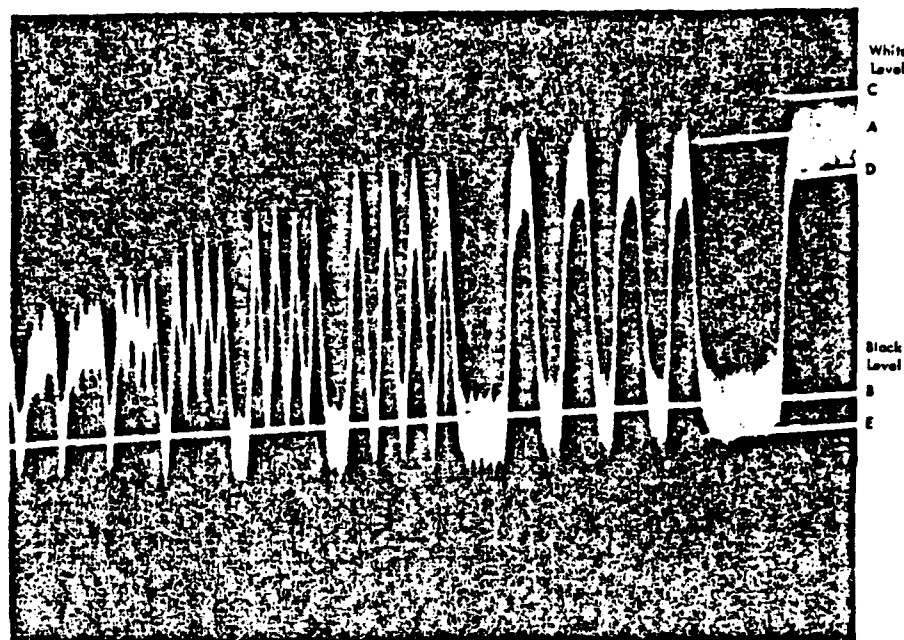


Figure 2.2 Standard Method of Determining SNR.

The maximum signal-to-noise ratio for television camera tubes is defined as the ratio of the peak-to-peak video signal to the rms noise, which can be written as

$$\text{SNR} = 6(\text{CE} - \text{DE})/\text{CD} . \quad (\text{eqn 2.7})$$

The dynamic range which is closely related to the noise of the imager can be defined as the ratio of the image output signal difference to the minimum output signal.

The maximum image output signal is obtained from the white background at just before signal saturation which depends on the aperture and on illumination of the chart. The minimum output signal is obtained from the dark bar at minimum aperture,  $F = 16$ .



The dynamic range then can be written as

$$DR = \frac{V_{max} - V_{min}}{V_{min}} \quad (\text{eqn 2.8})$$

### C. SPECTRAL RESPONSE

The term spectral responsivity (R) is used to describe the spectral sensitivity of the camera tube and is the ratio of the output signal voltage at given wavelength to the incident signal power.

Planck's law describes the spectral distribution of the radiation from a blackbody defined as the power radiated per unit wavelength interval at wavelength  $\lambda$  by unit area of a blackbody at temperature so called "spectral radiant emittance" ;

$$M_{bb}(\lambda, T) = \frac{2\pi hc^2}{\lambda^5} = \frac{1}{\exp(hc/\lambda kT) - 1} \quad (\text{eqn 2.9})$$

which may be written as

$$M_{bb}(\lambda, T) = \frac{c_1}{\lambda^5} = \frac{1}{\exp(c_2/\lambda T) - 1} \quad (\text{eqn 2.10})$$

where

$M_{bb}(\lambda, T)$  = blackbody spectral radiant emittance  
 $\left( \frac{W}{cm^2 \cdot \mu} \right)$

$\lambda$  = wavelength ( $\mu$ )

$T$  = absolute temperature ( $^{\circ}K$ )

$h$  = Planck's constant =  $6.6256 \times 10^{-34}$  (W.sec<sup>2</sup>)

$c$  = velocity of light =  $2.99793 \times 10^{10}$  (cm/sec)

$k$  = Boltzmann's constant

=  $1.38054 \times 10^{-23}$  (W.sec/ $^{\circ}K$ )

$c_1 = 2\pi hc^2 = 3.7415 \times 10^4$  (W $\mu^4$ /cm<sup>2</sup>)

$c_2 = hc/k = 1.43879 \times 10^4$  ( $^{\circ}K$ ).

The absolute value of the spectral radiant emittance depends on the width of the spectral interval. The spectral

interval is determined by the diffraction grating slit width, deflection angle, number of slits and wavelength in the spectroradiometer shown in Figure 2.3.

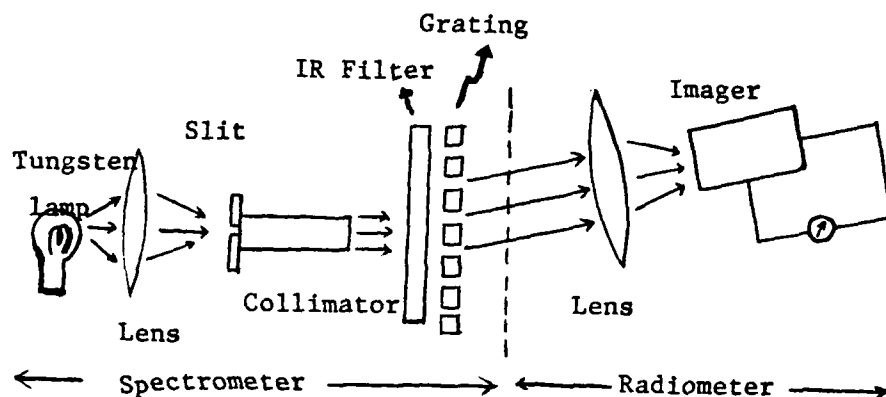


Figure 2.3 Elements of Spectroradiometer.

A spectroradiometer measures the spectral distribution of radiant flux in which the spectrometer provides radiant flux at wavelength intervals and a radiometer measures this flux passed through the imager. The wavelength of the flux passing through the imager is varied by the rotation of the TV camera.

The grating equation is needed to get the spectral interval which corresponds to the interval of two adjacent pixels (picture elements) in the camera tube. The well known grating equation for the normal incidence can be expressed as

$$m\lambda = a \sin \theta_m \quad (\text{eqn 2.11})$$

where

$m$  = order of image

$a$  = grating slit separation

$\theta_m$  = diffraction angle at order  $m$ .

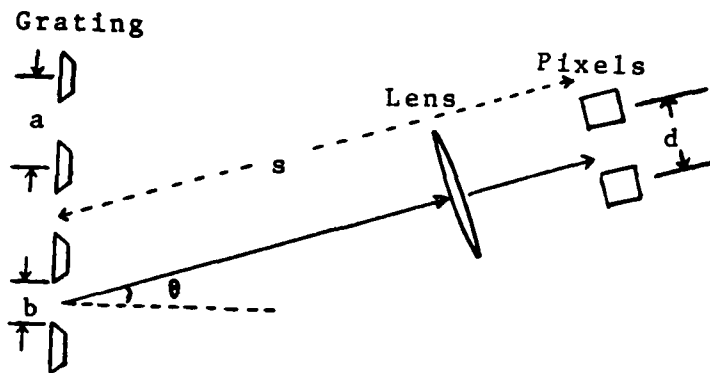


Figure 2.4 Diffraction Grating and Imager Array Pixels.

The deflection angle  $\theta = 0$  is defined by the  $m = 0$  (zeroth order white light image). The grating separates the various wavelengths according to the angle of deflection. The deflection angle as shown in Figure 2.4, determines the spectral interval to provide wavelength interval.

Differentiating the grating equation with respect to the deflection angle and setting  $m = 1$  for the first order image, the wavelength interval is

$$d\lambda = a \cos\theta d\theta \quad (\text{eqn 2.12})$$

where  $\theta$  is the angle of the imager from the undeflected  $m = 0$  as depicted in Figure 2.4. Replacing  $d\lambda$  by  $\Delta\lambda$  and  $d\theta$  by  $\Delta\theta$  we get spectral wavelength interval relation as

$$\Delta\lambda = a \cos\theta \Delta\theta . \quad (\text{eqn 2.13})$$

Using the small angle approximation, the angular resolution for the diode array can be defined by

$$\Delta\theta = \frac{d}{s} \quad (\text{eqn 2.14})$$

where

$d$  = separation of two pixels

$s$  = distance between grating and array pixel.

Substituting equation 2.14 back into equation 2.13, it becomes

$$\Delta\lambda = \frac{ad}{s} \cos\theta \quad (\text{eqn 2.15})$$

This is the wavelength interval as function of deflection angle. The maximum resolvable spatial frequency is 1/2 the pixel frequency in horizontal or vertical direction for the diode array and 1/2 to 1 of the reciprocal of the diameter of scanning beam spot for VIDICON. So, the separation of two pixels can be approximated to the half maximum of the contrast transfer function using the horizontal scan.

In pyrometry, one generally determines the brightness temperature of tungsten ribbon, that is the temperature of a blackbody with the same radiant intensity as the tungsten surface at a fixed wavelength.

The relation between brightness temperature, color temperature and true temperature for a tungsten ribbon filament lamp has been calculated based upon the emissivity of tungsten [Ref. 7]. The table including the luminance and various emissivity of tungsten was presented in Ref.8 and 9.

The brightness temperature is measured by the optical pyrometer and then converted into true temperature. The temperature used in this paper will represent the true temperature. The emissivity of the tungsten lamp at the wavelength and temperature must be multiplied by the spectral radiant emittance for a blackbody,  $M_{bb}(\lambda, T)$ , to get the spectral radiant emittance for a tungsten lamp,  $M_{tt}(\lambda, T)$ , which can be written as

$$M_{tt}(\lambda, T) = \epsilon(\lambda, T) M_{hb}(\lambda, T) . \quad (\text{eqn 2.16})$$

At a point where two or more optical fields overlap, the resultant optical field is the vector sum of the constituent fields which is applied to the electric field strength of the wave. Diffraction is treated by application of the principle of the superposition as described above. The wave disturbance at point p is the sum of the waves from all parts of the aperture acting as secondary sources, each giving a field at p as

$$E(\rho, t) = \frac{\epsilon_0}{\rho} e^{i(k\rho - \omega t)} . \quad (\text{eqn 2.17})$$

This process was formalized in the Fresnel-Kirchoff theory and the equation

$$E_p = - \frac{\epsilon_0 i}{\lambda} \iint_S \frac{e^{ik(\rho+r)}}{\rho r} \left[ \frac{\cos(\hat{n}, \hat{r}) - \cos(\hat{n}, \hat{\rho})}{2} \right] dS \quad (\text{eqn 2.18})$$

was developed in Ref. 10.

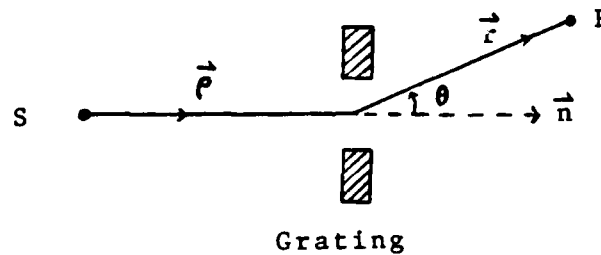


Figure 2.5 Geometry of Angle for Obliquity Factor.

This Fresnel-Kirchoff diffraction equation contains the angular dependence in the last term which is the obliquity factor. Since  $\hat{n}$  and  $\hat{\rho}$  are parallel, the angle  $(\hat{n}, \hat{\rho})$  is 0 and  $(\hat{n}, \hat{r})$  is  $\theta$  respectively. The geometry is shown in Figure 2.5. The obliquity factor then becomes

$$K(\theta) = \frac{\cos\theta + 1}{2} \quad . \quad (\text{eqn 2.19})$$

In the system constructed as Figure 2.3, only the size of the signal pattern changes and not its shape by moving the TV camera because the lens makes it far field. So, the Fraunhofer diffraction theory is applicable for this system to get the flux density on the TV camera. Remembering that the flux density is proportional to the square of the field strength, the obliquity factor then must be included in the flux density distribution function for multislit diffraction as

$$I(\theta) = I_0 \left( \frac{\sin\beta}{\beta} \right)^2 \left( \frac{\sin N\alpha}{\sin \alpha} \right)^2 \left( \frac{\cos\theta + 1}{2} \right)^2 \quad (\text{eqn 2.20})$$

where  $I$  is the flux density in the  $\theta=0$  direction which is equal to  $I(0)/N^2$ ,  $\alpha = \pi a \sin\theta/\lambda$  and  $\beta = \pi b \sin\theta/\lambda$  with refractive index of air equal to 1.

The flux density in the zero deflection angle passing through the filter is proportional to spectral radiant emittance of the light source and the transmittance of the filter which can be written as

$$I_0 \propto M_{tt}(\lambda, T) T(\lambda) \quad (\text{eqn 2.21})$$

where

$M_{tt}(\lambda, T)$  = spectral radiant emittance of tungsten

$T(\lambda)$  = transmittance of the slab (IR filter).

As we concentrate on the first order image, the principal maxima occurring  $m = 1$  or equivalently  $\alpha = \pi$  will be introduced in equation 2.20. The factor  $(\sin N\alpha / N \sin \alpha)^2$  is 1 at the principal maxima where  $\alpha = m\pi$ , ( $m = 0, 1, 2, 3, \dots$ ). Thus we can treat  $(\sin N\alpha / N \sin \alpha)$  a constant of 1. Substituting the equation 2.21 into the equation 2.20 we get the relative irradiance at any deflection angle as

$$I(\theta) = M_{tt}(\lambda, T) T(\lambda) \left( \frac{\sin \beta}{\beta} \right)^2 \left( \frac{\cos \theta + 1}{2} \right)^2 \quad (\text{eqn 2.22})$$

Finally, the relative spectral responsivity of the TV camera is obtained by the ratio of the output signal to the spectral irradiance formulated as

$$R = \frac{V}{I(\theta) \Delta \lambda} = \frac{V}{M_{tt}(\lambda, T) T(\lambda) \left( \frac{\sin \beta}{\beta} \right)^2 \left( \frac{\cos \theta + 1}{2} \right)^2 \Delta \lambda} \quad (\text{eqn 2.23})$$

where V is the signal output of the TV camera image.

### III. EXPERIMENTAL MEASUREMENTS AND RESULTS

#### A. EXPERIMENTAL APPARATUS

The experimental apparatus for this investigation consisted of three kinds of imaging devices, a Tektronix 468 Digital Storage Oscilloscope, an optical pyrometer and a grating spectrometer. The imaging devices required to conduct the performance measurement of the contrast sensitivity and spectral response were Charge Injection Device (CID), Charge Coupled Device (CCD) and VIDICON.

The Olympus lens having focal length of 50mm and F numbers of between 1.4 and 16 was used with these imagers.

The CCD compact solid state black and white TV camera consisted of solid state single chip image sensor, eliminating the pick-up tube and coil assembly. The built-in automatic control circuit produces the clear picture for low contrast such as Automatic Black Clamp circuit and Automatic Gain Control. This CCD (Model: Panasonic WV-CD10) has a scanning area of  $6.6 \times 8.8\text{mm}^2$  and 525 scanning lines.

The CID manufactured by General Electric Co.(4 TN 2505) and the VIDICON manufactured by CCTV corporation (CTC-2200) were used for the other two imagers, but their specifications are unknown.

A resolution chart was used for the object of these imagers. The pattern of this resolution chart was the alternating black and white bar having both horizontal and vertical bars. The image spatial frequency (line-pairs/mm) depends on the object distance from the lens as discussed in section II.

A Tektronix 468 Digital Storage Oscilloscope (DSO) was used to measure the output signal amplitude of the TV camera in conjunction with a TV monitor and the image of the TV camera was displayed on TV monitor. The TV camera signal was sent to 468 DSO to display the amplitude of the signal.



The 468 DSO has a digital storage circuitry for the acquisition of signals and displays the acquired signal with a bright, flicker-free trace.

For the measurement of spectral response of the imager, an optical pyrometer (8630 series), a tungsten ribbon filament lamp, a spectrometer, a diffraction grating (10000 lines/inch) and a 468 DSO were set up.

Figure 3.1 shows a block diagram of the experimental set-up used for the measurement of spectral response in the near infrared wavelength region.

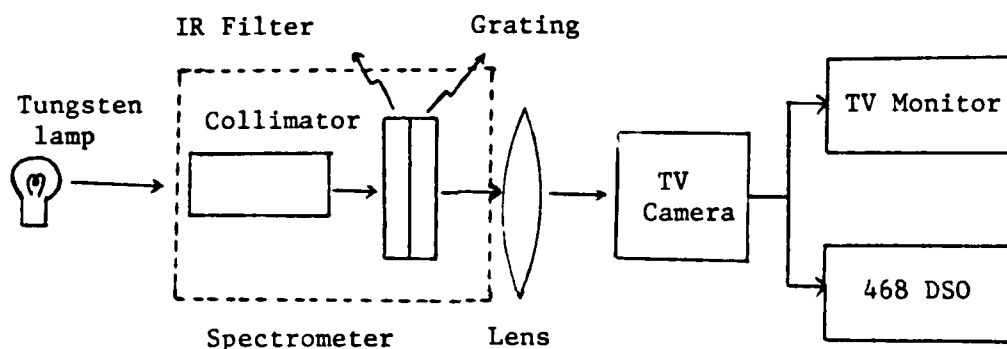


Figure 3.1 Spectral Response Measurement Set-up.

An optical pyrometer (Model: 8632-C) was used to measure the brightness temperature of the tungsten light source. The brightness temperature could be measured at three ranges 775-1225 °C, 1075-1750 °C and 1500-2800 °C which can be converted into true temperature as described in section II. The brightness temperature was measured by matching the brightness when the filament appears to merge with or disappear into the image of the hot object. The true temperature of 2520 °K was used for the spectral response measurement and comparison of all three TV cameras which is the maximum temperature to get the maximum intensity without saturation for the most sensitive camera, CID.

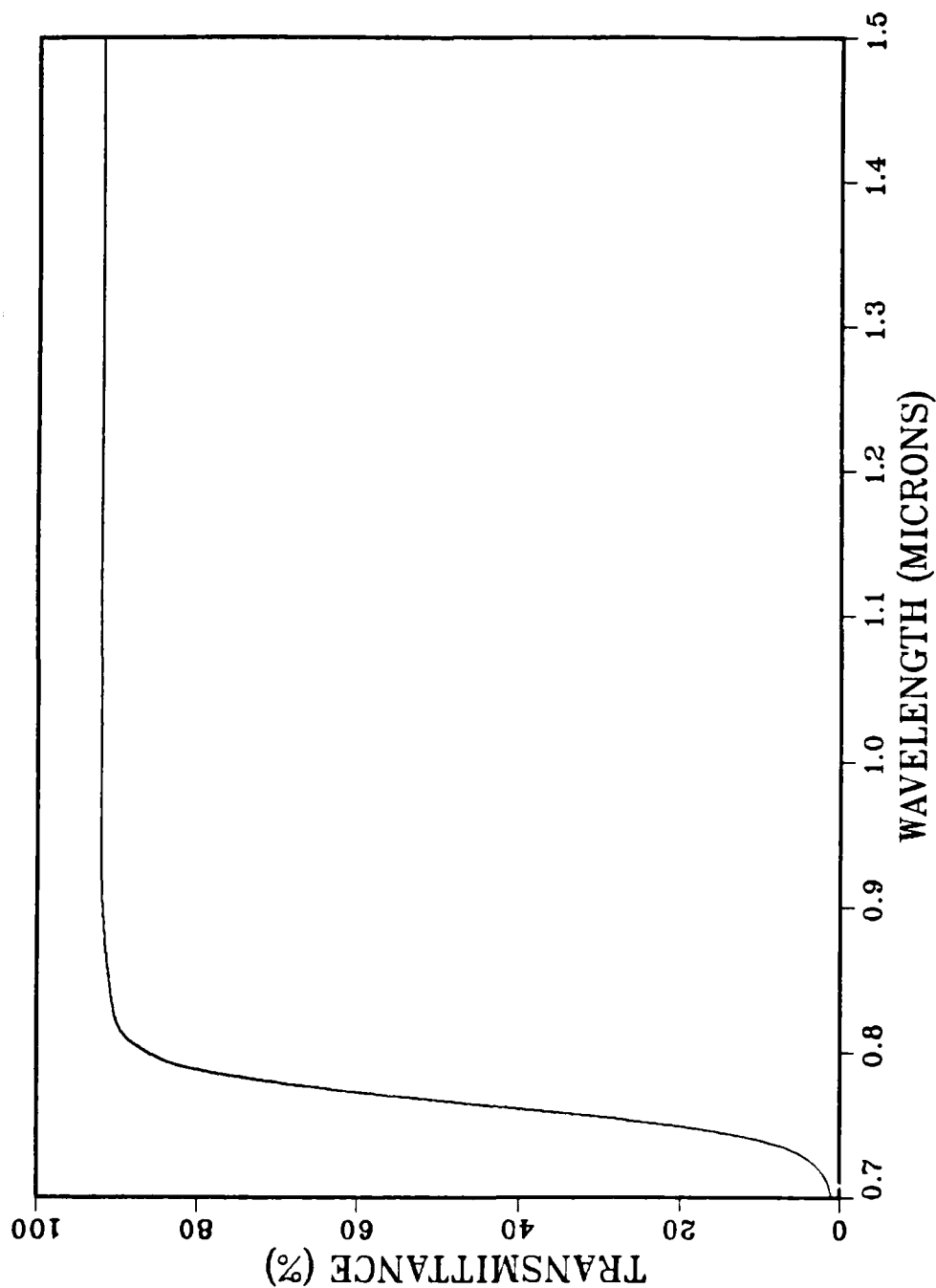


Figure 3.2 Transmittance of the IR Filter.

In the spectrometer, the telescope was removed and replaced with camera and lens. The camera needs to see the spectrum lines at various angles to get the intensity distribution by rotating. The infrared filter and the diffraction grating are fixed close together normal to the incident light. An infrared filter was used to remove the visible light which produces the second order visible spectrum on top of the first order spectrum of infrared region. Its transmittance curve was presented in Figure 3.2. The adjustable supporting plate for the TV camera was attached in place of the telescope. The spacing from the grating to the camera lens was 21.3 cm.

The image signal is sent to the TV monitor and then to the 468 DSO to measure the TV spectral response at each deflection angle. The measured angle corresponds to a particular wavelength of the spectrum. The TV camera views a portion of the spectrum at each angle. The voltage readings are taken at the center of the viewing area, i.e. at the center of the horizontal scan.

## B. CONTRAST SENSITIVITY

### 1. Signal-to-Noise Ratio (SNR)

Usually the SNR is expressed in decibels in terms of the noise in a particular wavelength. There are various sources of noise which interfere with the precise measurement of the signal current. The primary temporal noise sources in imagers are amplifier noise, capacitor reset noise and dark current noise.

The noise of all TV cameras was measured based on this primary noise neglecting the noise of the 468 DSO since it was negligibly low comparing to the imager noise.

To get the noise without a signal, the lens of the camera is covered. This noise signal is displayed and digitized on 468 DSO. The digitized noise is measured with 300 samples for each camera to get rms value of the noise. The rms noise was calculated by standard deviation value to be

8.85mV for CID, 12.97mV for VIDICON and 33.05mV for CCD. These noise pictures are presented in Figure 3.3, 3.4 and 3.5 with the amplitude of 50mV per division. Two tungsten lamps, controlled by a Variac, were used for the light source and white background of the resolution chart was used to get the maximum output signal. One of the most important factors varying the output signal is the flux density. The flux density (microwatts/cm<sup>2</sup>) of the incident light on the camera was measured using a silicon pin photodiode (Model:PIN-10D). A silicon pin photodiode placed on the camera lens looking at the object sensed the incident light.

The signal and the noise were measured by the standard method as discussed in section II. The maximum signal was obtained by the maximum intensity of light at just before saturation of the white background signal on the oscilloscope. Then the maximum SNR was determined with the help of equation 2.7 and it may be expressed in decibels by taking  $10 \log(\text{SNR})$ . The calculated maximum SNR at  $F=1.4$  was tabulated in Table I where  $V_w$  is the signal due to the white background and  $V_b$  is the signal due to the black bar.

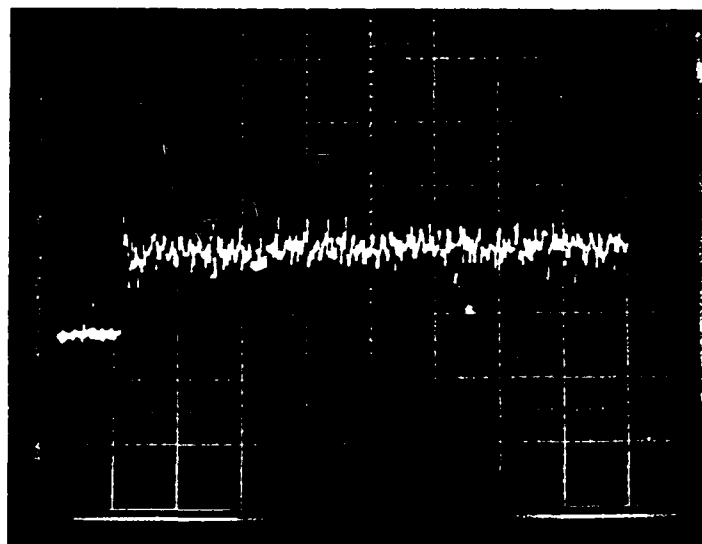


Figure 3.3 Noise without a Signal(50mV/div): CID.

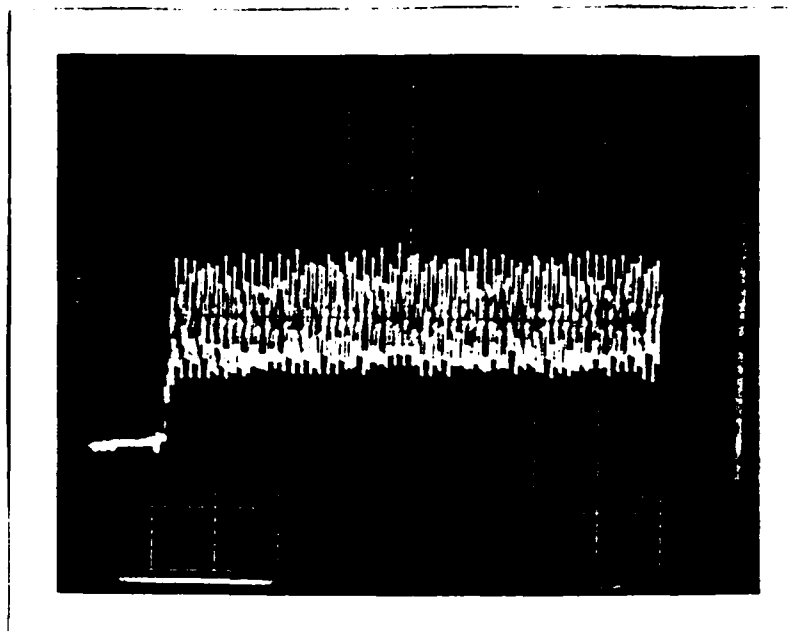


Figure 3.4 Noise without a Signal(50mV/div): CCD.

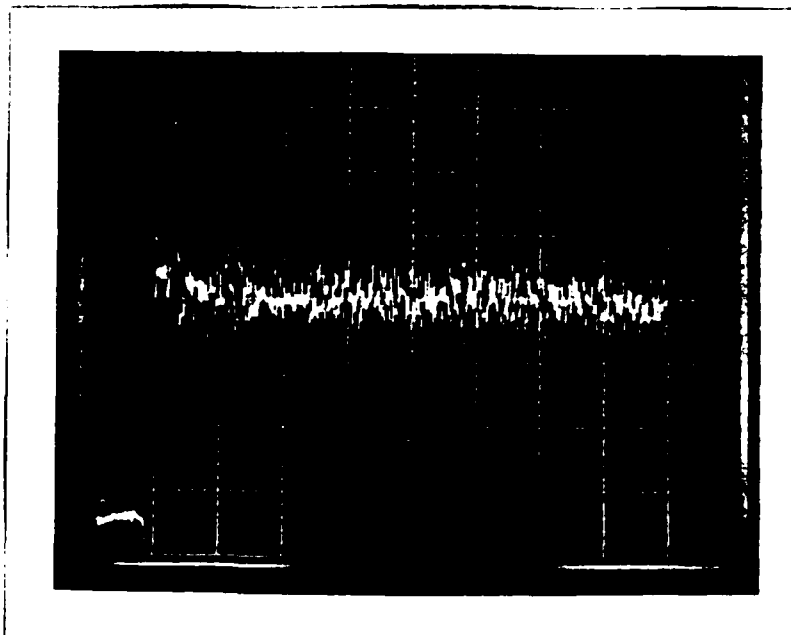


Figure 3.5 Noise without a Signal(50mV/div): VIDICON.

TABLE I  
MAXIMUM SIGNAL-TO-NOISE RATIO

TV cameras	Flux density on pin diode ( $\mu\text{W} / \text{cm}^2$ )	$V_w - V_b$ (mV)	Maximum SNR (decibels)
CCD	2.17	360	15.14
VIDICON	5.02	440	20.08
CID	0.43	460	21.93

## 2. Dynamic Range

The dynamic range is greatly affected by the imager noise since it determines the sensitivity of the device. Two aperture sizes and the minimum irradiance are required for this measurement.

For the first step, the minimum aperture size ( $F1=16$ ) of the lens and the minimum irradiance of the tungsten light source were set to be able to see the minimum resolvable image on the TV screen. The output voltage was measured then at this condition on 468 DSO which is the minimum. The maximum output voltage was measured at  $F2$  where the signal output begins to saturate. This was done by increasing the aperture size up to that limit. The irradiance of the tungsten light source, however, kept fixed.

TABLE II  
DYNAMIC RANGE COMPARISON

TV cameras	F1	F2	$V_{min}$ at F1(mV)	$V_{max}-V_{min}$ at F2(mV)	Dynamic Range
VIDICON	16	1.4	185	330	1.78
CCD	16	2.5	90	340	3.78
CID	16	1.4	60	435	7.25

Finally, the dynamic range is determined by the ratio of the output voltage difference at  $F1$  to the minimum

output voltage at F2 as expressed in equation 2.8 . The output voltage difference is the difference between the maximum due to the background and the minimum due to the black bar of the resolution chart.

The F numbers making the signal saturation may be different for each camera because their contrast sensitivities are different. The resulting values are compared and tabulated in Table II.

### 3. Linearity

The study of linearity of TV camera can be useful for the signal proportionality to the incident light and for the device behavior.

The storage mode of 468 DSO was used to measure the mean amplitude of the charge signal and the maximum value of that signal by the irradiance of the tungsten light source at each F number.

The object distance of 40cm and the radiant flux of 4.46 microwatts were used to get the most reasonable data for the output signal comparison of the three cameras.

Since the entrance pupil diameter of the lens is the focal length per F number, the area of the entrance pupil is inversely proportional to the square of the F number. Hence, the linearity of the TV camera signal can be obtained from the maximum signal output as function of the entrance pupil area. The maximum signal output was measured in the same manner as in the dynamic range at each F numbers . The measured data were plotted in Figure 3.6.

The linearity of TV camera signal can be obtained only at certain region of the aperture that is F number of 16 through 9 for these three cameras. The output signal is nearly constant below the F number of 9. The linearity for the TV camera signal was presented in Figure 3.7.

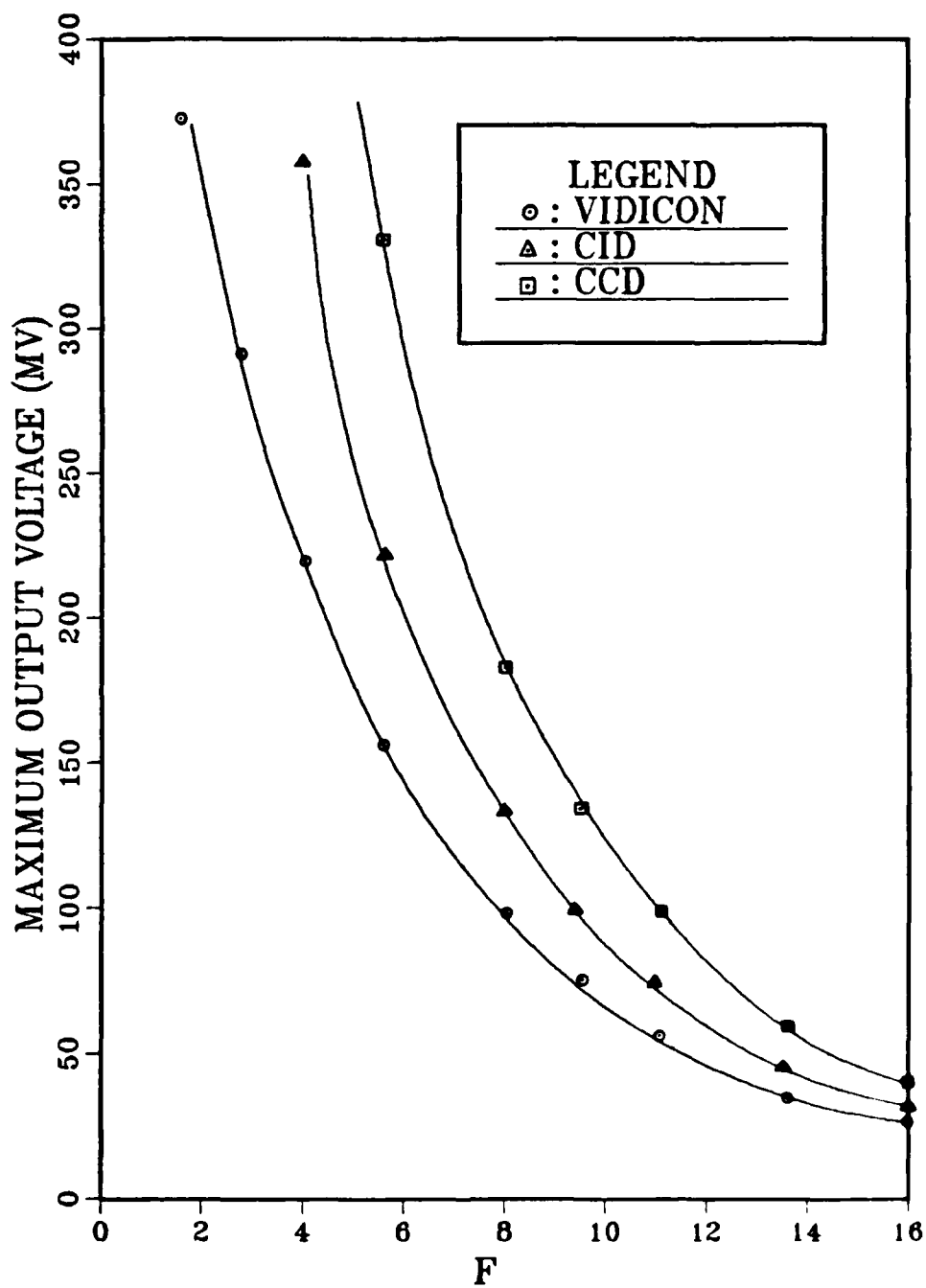


Figure 3.6 The Maximum Output Voltage vs F Number.



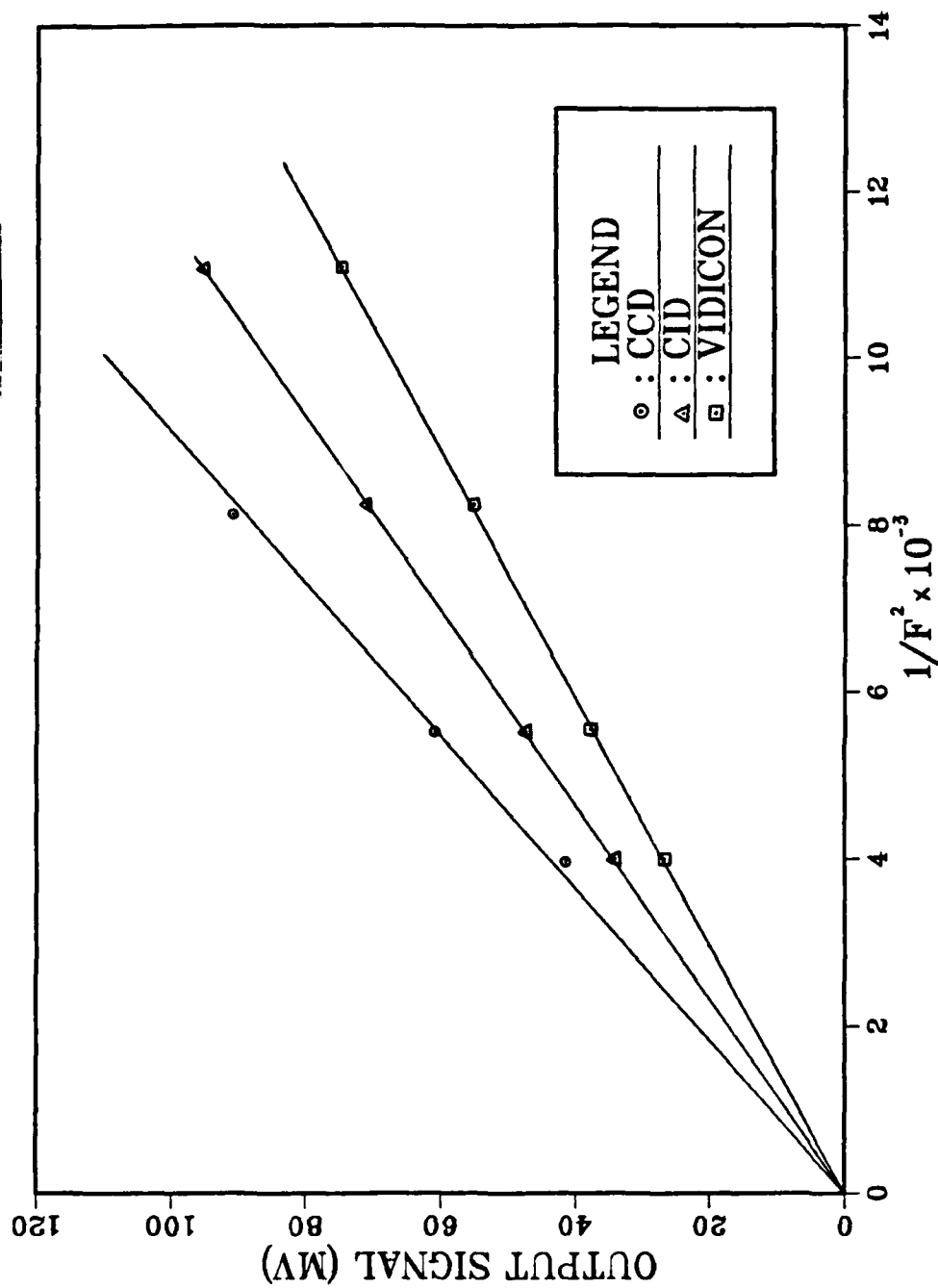


Figure 3.7 Linearity of TV Camera Signal.

#### 4. Contrast Transfer Function (CTF)

It is preferable to measure the resolution performance of camera tubes in terms of CTF characteristics. Contrast here is defined as the ratio of the image difference in luminance between the dark bar and its background to the luminance of the background.

A black and white bar chart was constructed for the object of the TV camera to get the square wave spatial frequency amplitude response making the object distance of 83.5cm and the lux density of 0.93microwatts/cm<sup>2</sup> for all TV cameras used in this research. Only the F number was different because of different resolution limit which was  $F = 4.0$  for CID,  $F = 1.4$  for both CCD and VIDICON.

The bar chart having 12 different elements was used to scan horizontally and vertically together and their object spatial frequency range was 0 through 2.0 line-pairs/mm. The image spatial frequency range at the object distance of 83.5 cm was calculated to be 0 through 31.4 line-pairs/mm with the help of equation 2.5.

The image output signal was measured from 468 DSO moving the chart to get the CTF at equal luminance keeping the tungsten light source and TV camera fixed. The measuring point of CTF was controlled manually by either positioning the center of image to the center of oscilloscope or to the center of TV monitor.

In measurement of the CTF, the maximum output signal was measured by the background portion and the minimum output signal by the dark bar of an element. The maximum output signal was reduced while the minimum value increases as the spatial frequency of the element increases. The CTF for each resolution element was calculated with these measured output signals using the equation expressed in section II. The measured CTF curves were plotted for both horizontal and vertical scan in Figure 3.8 through 3.10 as a function of image spatial frequency. The resolving

capability at the scene contrast values for each camera may be determined from the CTF curves.

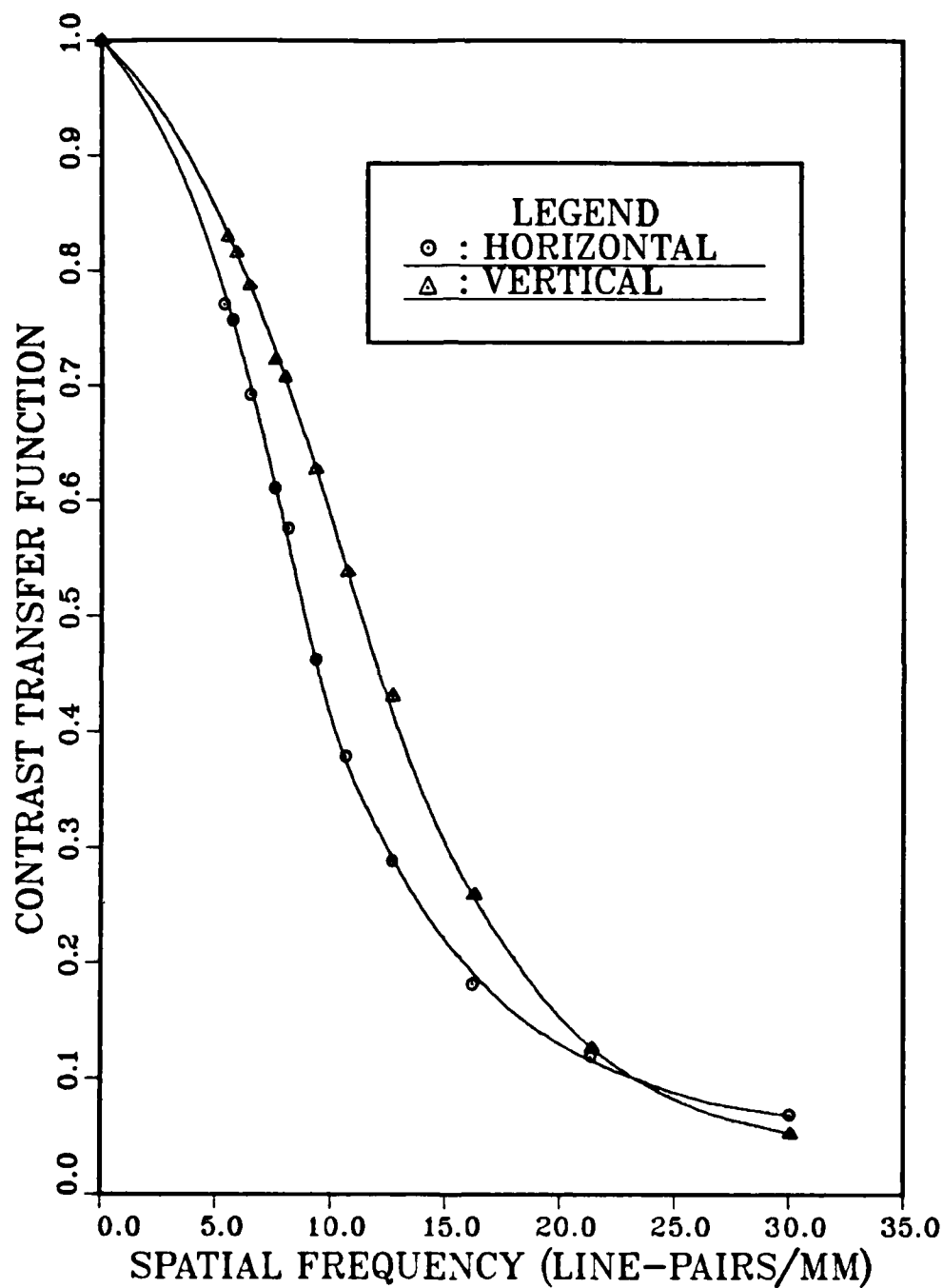


Figure 3.8 CTF for CID at  $F=4.0$  and  $O=83.5$  cm.

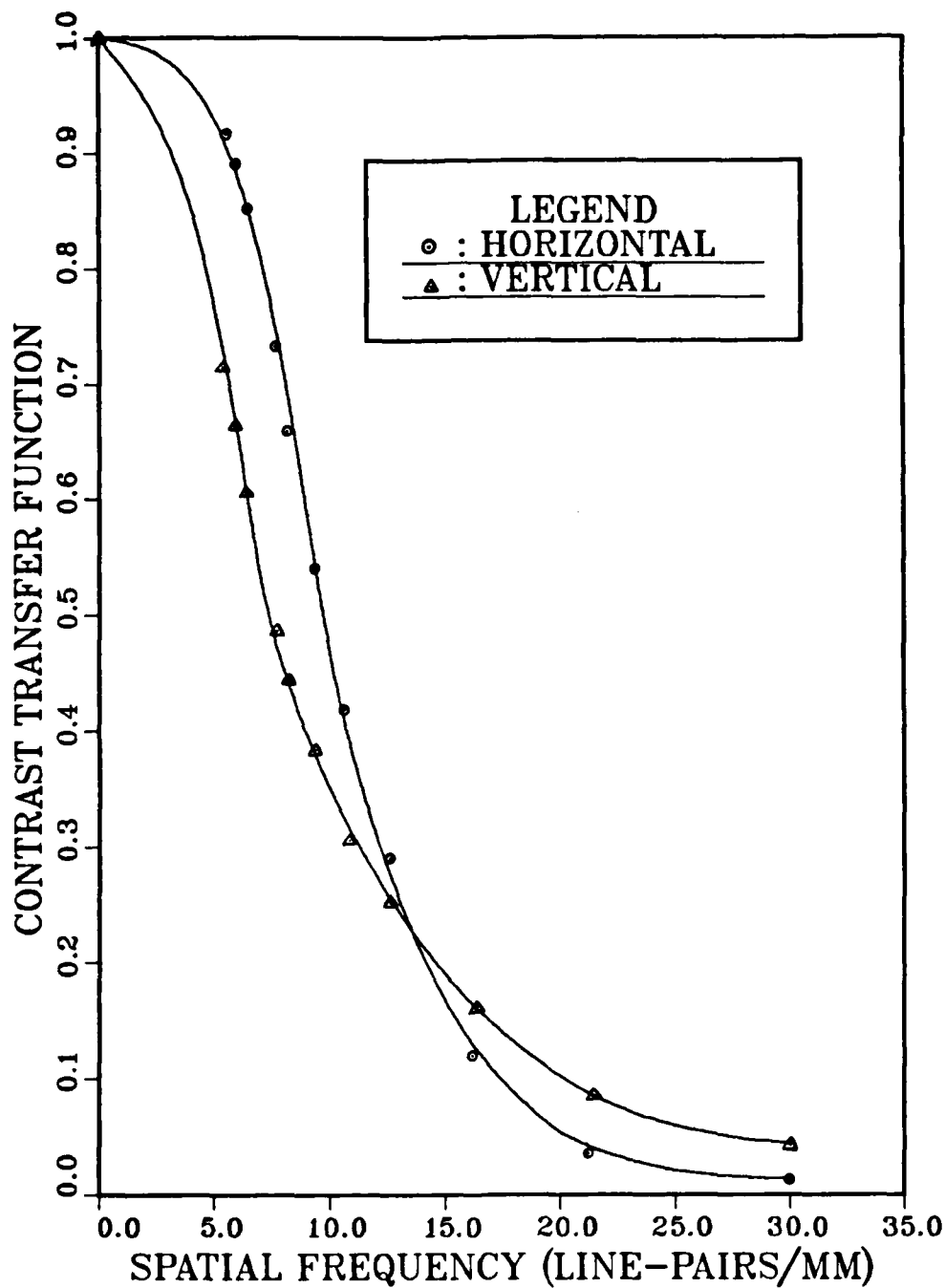


Figure 3.9 CTF for CCD at  $F=1.4$  and  $O=83.5$  cm.

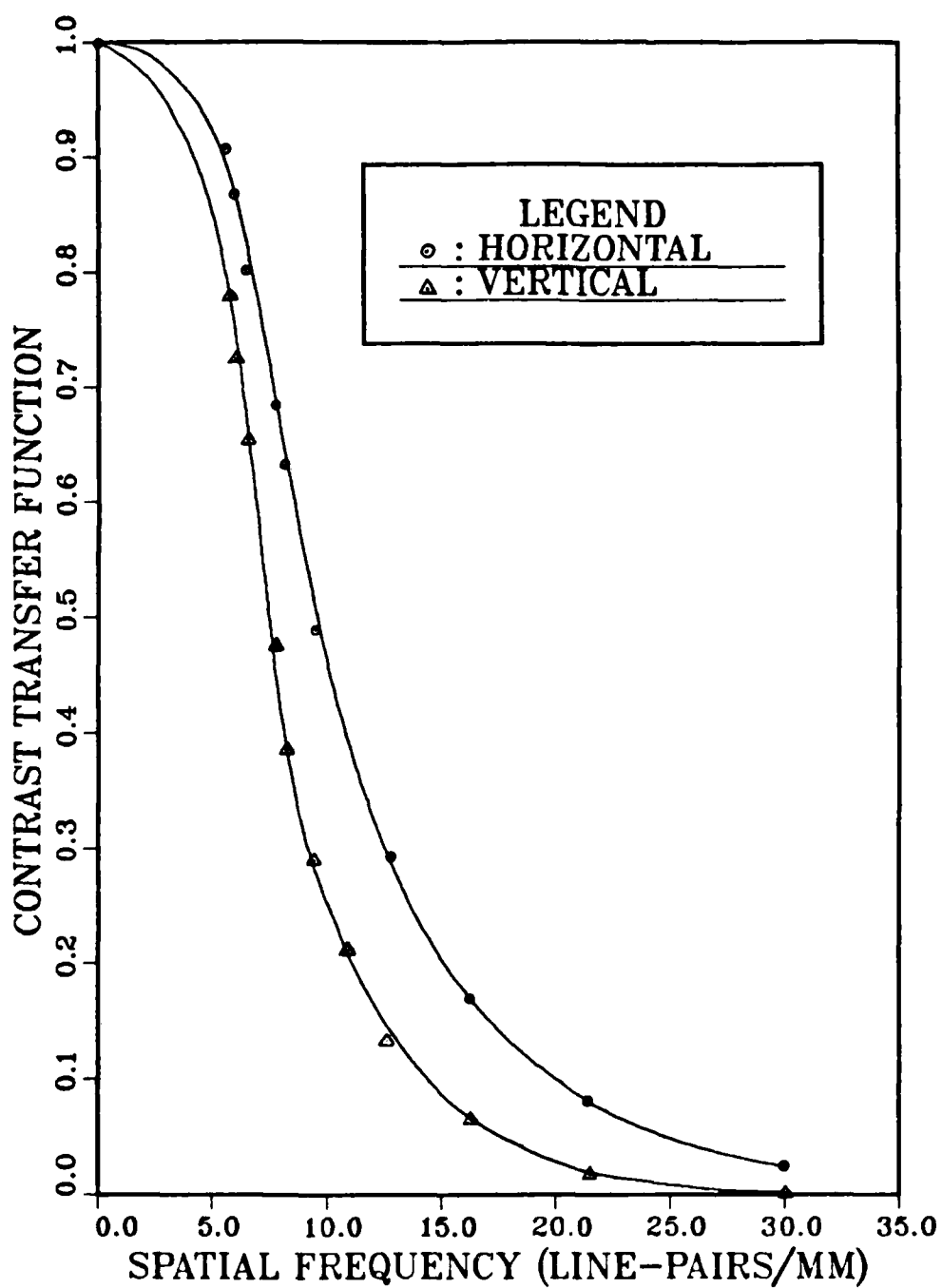


Figure 3.10 CTF for VIDICON at  $F=1.4$  and  $O=83.5$  cm.

## C. SPECTRAL RESPONSE

### 1. Spectral Radiant Emittance

Planck's blackbody function provides a good approximation of the true radiation of a tungsten filament lamp in the range of visible sensitivity, but outside the visible range the approximation is less accurate because of variations in the emissivity of tungsten with the temperature and wavelength. Emissivity is a function of the type of material and its surface finish and it can vary with wavelength and with temperature of the material. In this paper, the spectral radiant emittance is evaluated by use of tungsten emissivity data.

The analysis of TV camera spectral response was started with the measurement of brightness temperature of the tungsten filament light source using the optical pyrometer. The measured brightness temperature was converted into the true temperature with the help of table presented in Ref.8.

As the emissivity depends on both the temperature and the wavelength, the wavelength of spectrum must be measured in addition to the temperature.

TABLE III  
THE VISIBLE LINES IN THE SPECTRUM OF A MERCURY ARC

Color	Wavelength (angstroms)	Deflection angle (degrees)
Violet	4047	9.231
Blue	4358	9.947
Bluegreen	4916	11.237
Green	5461	12.501
Yellow 1	5770	13.221
Yellow 2	5791	13.270

A diffraction grating (10000 lines/inch) was used to obtain the spectrum. A mercury arc was used for the light source with the spectrometer to calibrate the grating. The

wavelength of the six visible lines and corresponding deflection angle in the first order image to be used are presented in table III [Ref. 11].

The actual grating slit separation ( $a$ ) was determined to be 2.523 micrometers with the help of equation 2.11 and the table III. A He-Ne laser (632.8 nm) was used on the spectrometer for the light source to determine the slit width. The flux density  $I(0)$  and  $I(\theta)$  were measured passing through the grating and the television camera. The slit width then was determined to be 2.085 micrometers using the equation 2.20 .

The emissivity of the tungsten lamp was determined from the table presented in Ref. 9. The emissivity versus wavelength was presented in Figure 3.11 for the temperature of 2520 °K. The blackbody spectral radiant emittance was calculated in the near infrared region (0.7-1.5 micrometers) at 2520 °K and plotted in Figure 3.12. The tungsten spectral radiant emittance was determined by multiplying the blackbody spectral radiant emittance by the emissivity of tungsten as shown in Figure 3.13.

## 2. Responsivity of TV Camera

The spectral responsivity of an imager provides the response to the radiant flux in a very narrow spectral band centered about any desired wavelength. One way of describing the spectral response of an imager is to plot its relative response as a function of wavelength for a constant radiant flux per unit wavelength. The flux density and the responsivity determined in this paper are the relative values.

The light from the tungsten filament lamp was focused on the entrance of the collimator and the beam from the collimator fell normally on the infrared filter. The light which passed through the filter was incident on the diffraction grating which separated it into its spectral components.

The TV camera and lens were positioned on the zero order line to determine the 'zero' angle of the grating spectrometer with the zero order image in the center of the display monitor and the 468 DS0. The TV camera was then rotated into first order spectrum in the near infrared region. The measured deflection angle was converted into the wavelength using equation 2.11 and plotted in Figure 3.14. The output signal was measured in millivolts from 468 DS0 in the near infrared region. The curve was plotted in Figure 3.15.

The array pixel separation ( $d$ ) in the camera is obtained from the image spatial frequency at half maximum value of horizontal scanned CTF for each camera. The resulting values are 0.1124 mm for CID, 0.1031 mm for CCD and 0.1045 mm for VIDICON. The distances from grating to pixel was 26.3cm (Fig 2.3). This value will be used for determination of wavelength interval.

Finally, the responsivity of TV camera is calculated with the help of equation 2.23. The resulting curves were presented in Figure 3.16.



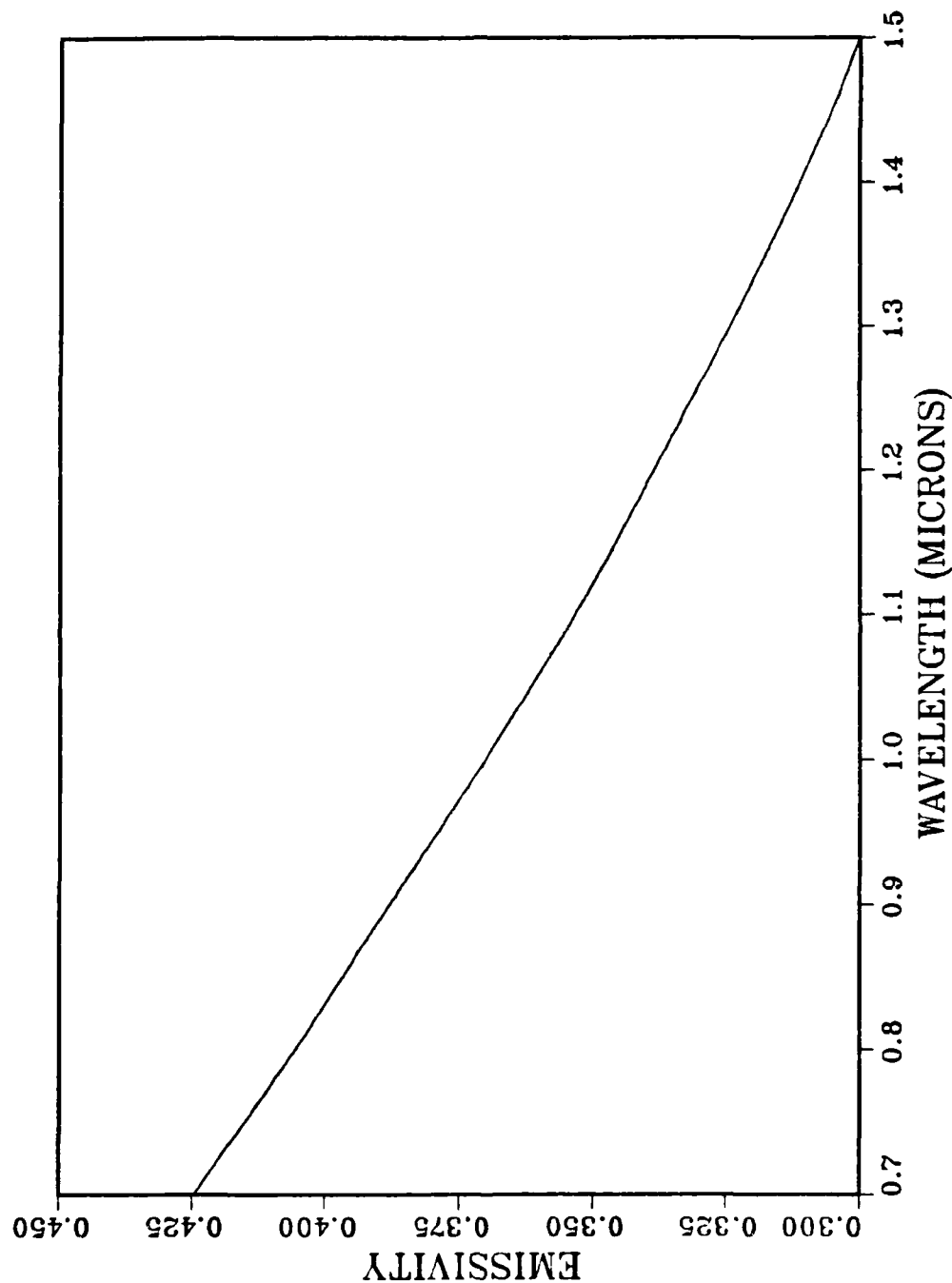


Figure 3.11 Tungsten Lamp Emissivity ( $T=2520^{\circ}\text{K}$ ).

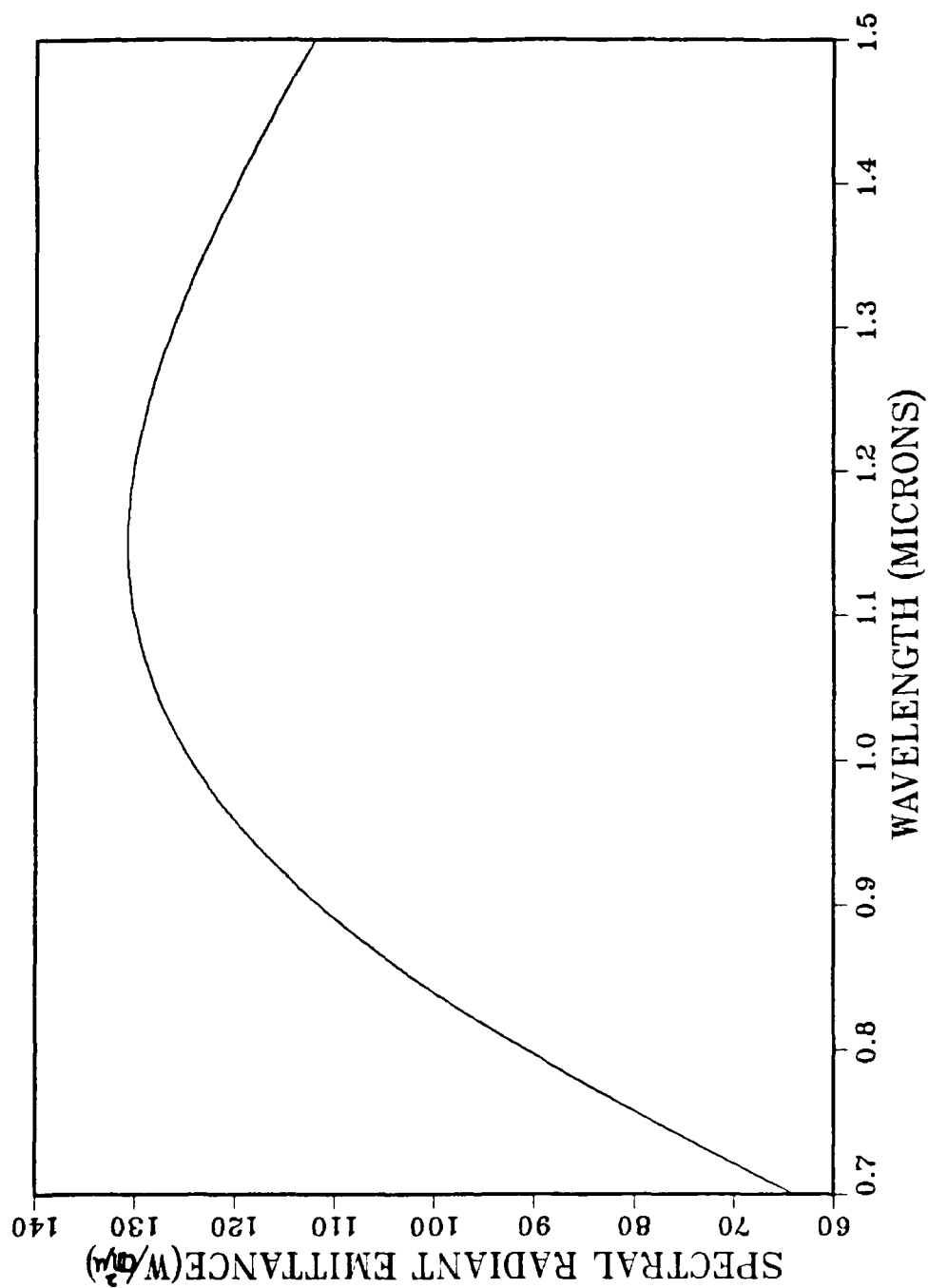


Figure 3.12 Blackbody Spectral Radiant Emittance ( $T=2520\text{ }^{\circ}\text{K}$ ).

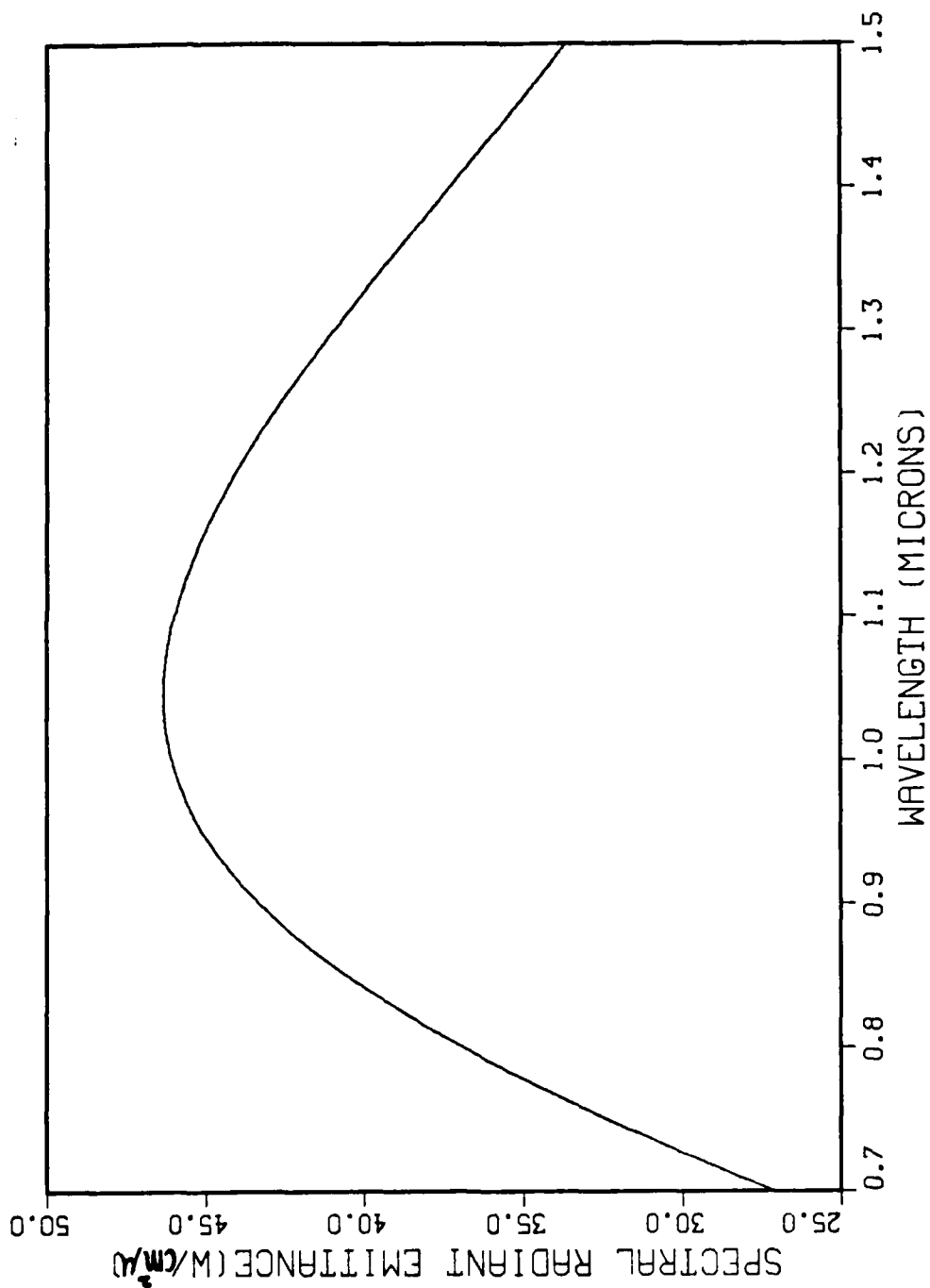


Figure 3.13 Tungsten Spectral Radiant Emittance ( $T=2520\text{ }^{\circ}\text{K}$ ).

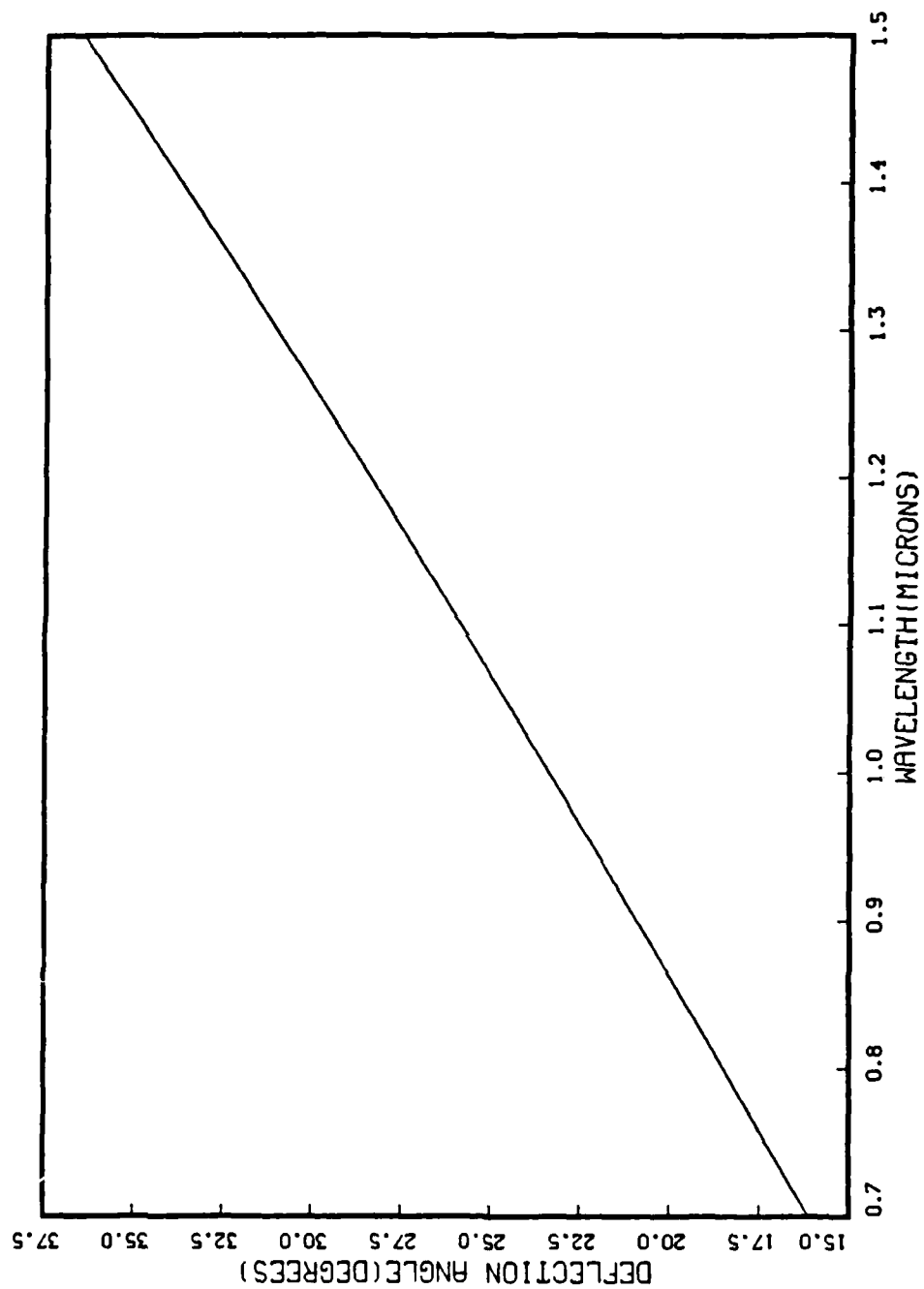


Figure 3.14 Deflection Angle vs Wavelength.

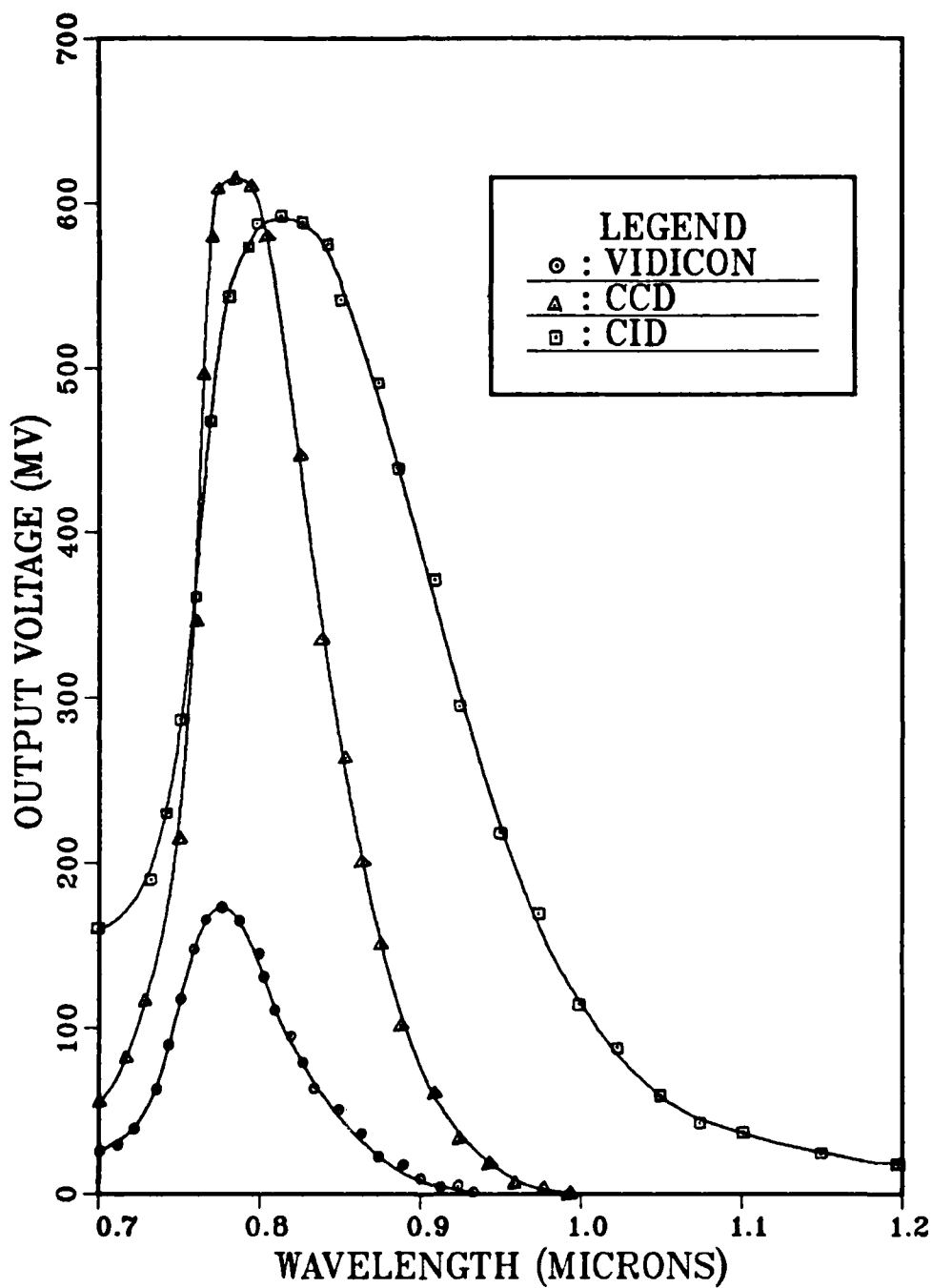


Figure 3.15 Signal Output vs Wavelength.

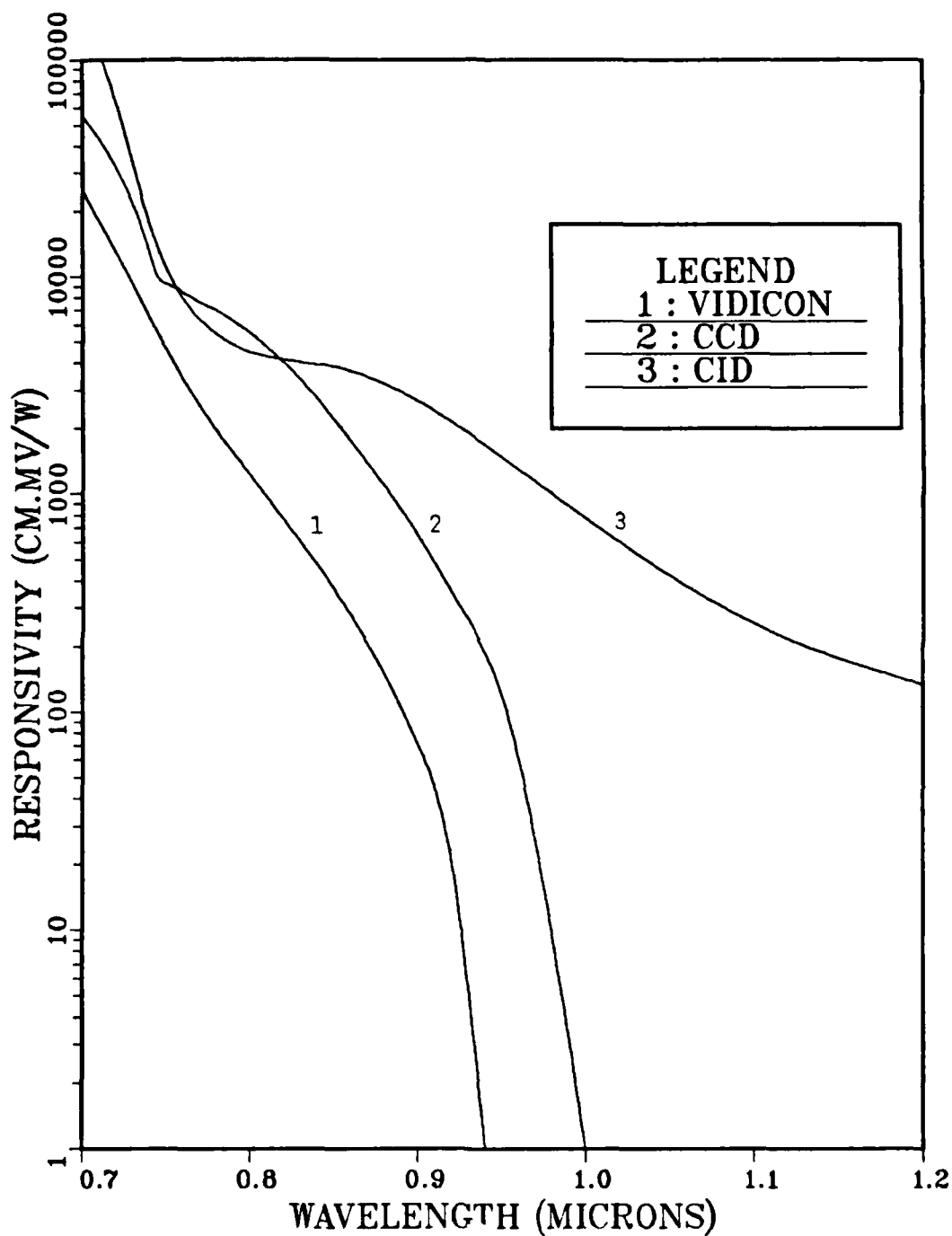


Figure 3.16 Responsivity of TV Camera.

#### IV. CONCLUSIONS

From the survey of three TV cameras, the following general conclusions can be drawn.

- 1) The limiting resolution values for horizontal scan corresponding to a CTF of three percent were determined to be 23 line-pairs/mm for CCD, 28.4 line-pairs/mm for VIDICON and its value for CID could not be determined, but was much higher than these values.
- 2) The solid-state imager CID is a more sensitive device, having relatively lower noise and higher dynamic range than the CCD or VIDICON. The CID has high capability of resolution at the actual scene contrast values of 30 per cent, or less. Thus, the CID is more appropriate for low light level applications compared to the other two imagers.
- 3) Compared to the VIDICON or CID, the CCD has better resolving capability at the scene contrast values of 50 per cent, or more.
- 4) The resolution and the contrast sensitivity of an imager are greatly affected by the radiant flux.
- 5) The spectral response for CID is much broader than the other imagers and extends into the entire near infrared with response of 134 cm.mV/W at 1.2 micrometers.
- 6) The cutoff wavelengths were determined to be 1.00 micrometers for CCD and 0.94 micrometers for VIDICON, but both were much shorter than that of CID.
- 7) It is recommended that a resolution chart with larger scale be used than the object spatial frequency of 5 line-pairs/mm to get more accurate CTF curve at the low image spatial frequency region.

## LIST OF REFERENCES

1. Electro-Optics Handbook, EOH -11, RCA Corporation, Lancaster, PA., 1974.
2. Weimer, P., Forgue, S. and Goodrich, R., Vidicon-Photoconductive Camera Tube, Electronics, pp. 70-73, McGraw-Hill Book Co., May 1950.
3. Burke, H. K. and Michon, G. J., "Charge-Injection Imaging: Operating Technics and Performance Characteristics," IEEE Journal of Solid-State Circuits, Vol. SC-11, No. 1, pp. 121-127, February 1976.
4. Wolfe, W. L. and Zissis, G. J., The Infrared Handbook, Ch. 13, Office of Naval Research, Dept. of the Navy, Washington D.C., 1978.
5. Miller, I. and Fuend, J. E., Probability and Statistics for Engineers, 2d ed., Ch. 5, Prentice-Hall Inc., New Jersey, 1977.
6. Biberman, L. M. and Nudelman, S., Photoelectronic Imaging Devices, V. 2, pp. 95-97, Plenum press, New York-London, 1971.
7. Rutgers, G. A. W. and De Vos, J. C., "Relation Between Brightness Temperature, True Temperature and Color Temperature of Tungsten. Luminance of Tungsten," Physica, V. 20, p. 715, October 1954.
8. Rogers, W. F. and Wensel, H. T., American Institute of Physics Handbook, 2d ed., McGraw-Hill Book Co. Inc., N.Y., p. 6-168, 1963.
9. Weast, R. C., Handbook of Chemistry and Physics, 54th ed., p. E-217, CRC Press, 1973-1974.
10. Hecht, E. and Zajac, A., Optics, pp. 364-392, Addison-Wesley Pub. Co., 1979.
11. Valasek, J., Introduction to Theoretical and Experimental Optics, p. 357, John Wiley and Sons, Inc., New York, 1949.



# INITIAL DISTRIBUTION LIST

	No.	Copies
1. Defense Technical Information Center Cameron Station Alexandria, Virginia 22304-6145	2	
2. Library, Code 0142 Naval Postgraduate School Monterey, California 93943-5002	2	
3. Department Chairman, Code 61 Department of Physics Naval Postgraduate School Monterey, California 93943-5100	2	
4. Professor E. A. Milne, Code 61Mn Department of Physics Naval Postgraduate School Monterey, California 93943-5100	2	
5. Chief of Naval Operations Republic of Korea Naval Headquarters Sin Gil-Dong Young Deung Po-Gu Seoul, Republic of Korea	2	
6. Library Officer Naval Academy Chinhae, Republic of Korea	1	
7. Yim, Chang Ho SMC 2425 NPS Monterey, California 93943	1	
8. Kim, Ku Hyun SMC 1076 NPS Monterey, California 93943	1	
9. Kim, Young Soo #70, 2-Ga Dong Dae Sin-Dong Seo-Gu Busan, Republic of Korea	5	

END

FILMED

3

-86

DTIC